

## Supplementary Information for

# Sulfur Edge in Molybdenum Disulfide Nanosheets Achieves Efficient Uranium Binding and Electrocatalytic Extraction in Seawater

### *Experimental Details*

#### **Chemicals and materials.**

**Synthesis of pristine MoS<sub>2</sub> and S-terminated MoS<sub>2</sub> nanosheets.** The pristine MoS<sub>2</sub> nanosheets and S-terminated MoS<sub>2</sub> nanosheets was fabricated as described before.<sup>1</sup> In detail, for the synthesis of pristine MoS<sub>2</sub> nanosheets, 1 mmol hexaammonium heptamolybdate tetrahydrate ((NH<sub>4</sub>)<sub>6</sub>Mo<sub>7</sub>O<sub>24</sub>·4H<sub>2</sub>O, HHT, 7 mmol Mo) and 14 mmol thiourea (Mo:S ratio = 1:2) were dissolved in 35 mL deionized water under vigorous stirring to form a homogeneous solution. Then, the solution was transferred into a 45 mL Teflon-lined stainless steel autoclave, maintained at 220 °C for 18 h, and allowed to cool to room temperature naturally. The final product was washed with water and absolute ethanol for several times and dried at 60 °C under vacuum. The S-terminated MoS<sub>2</sub> nanosheets was synthesized by adjust the ratio of thiourea (Mo:S ratio = 1:4).

**Electrode preparation.** Carbon-graphite felt was cut into 1 × 2 cm quadrate shapes as electrode substrates. 5 mg of the as-prepared S-terminated MoS<sub>2</sub> nanosheets, 5 mg of active carbon, and 35 μL Nafion solution (5 wt%) were dispersed in 2 mL of ethanol by sonicating for 1 h to form a homogeneous ink. The mixture was then uniformly spread on carbon-graphite fiber to prepare the working electrode. The platinum wire served as the counter electrode.

**Uranium extraction experiment.** Spiked uranium solutions were made by dissolving uranyl nitrate salt (VWR, reagent grade) into real seawater to different concentrations. In each electrodeposition experiment, 100 ml of spiked uranium solution was used. The absorbed uranium mass was calculated by comparing the uranium concentration difference before and after adsorption.

**Computational details.** We have performed the DFT calculations in our system by using the Vienna ab initio simulation package (VASP).<sup>[2]</sup> The PBE<sup>[3]</sup> functional which is used for

electronic exchange and correlation. The projector augmented wave<sup>[4]</sup> method was adopted to describe the interactions between the ion cores and valence electrons. In our calculation, the monolayer MoS<sub>2</sub> model was constructed by adding a 15 Å thick vacuum to the y-direction and 10 Å of vacuum in the z-direction to avoid interactions between adjacent layers. A kinetic energy cutoff for this system was set to 450 eV. The Brillouin zone was sampled by the Monkhorst-Pack scheme<sup>[5]</sup> using a 2 × 1 × 1 k-point grid. For this system, the total electronic energies and the forces on the per atoms were converged to 10<sup>-5</sup> eV and 0.02 eV/Å respectively. The DFT-D3<sup>[6]</sup> correction method was adopted to account for van der Waals (vdW) interaction.

The adsorption energy ( $\Delta E_{\text{ads}}$ ) is calculated as:

$$E_{\text{ads}} = E_{\text{adsorbate}/\text{MoS}_2} - (E_{\text{adsorbate}} + E_{\text{MoS}_2})$$

where  $E_{\text{adsorbate}/\text{MoS}_2}$ ,  $E_{\text{adsorbate}}$ , and  $E_{\text{MoS}_2}$  are the total energies of MoS<sub>2</sub> with adsorbate, isolated adsorbate, and MoS<sub>2</sub>, respectively.

**Characterizations.** Characterizations Scanning electron microscopy (SEM, Ultra55, Carl zeissNTS GmbH, Germany) was utilized to investigate the morphology of the electrocatalyst. Transmission electron microscopy (TEM) and high-resolution TEM images (HRTEM) were performed by using afieldemission high-resolution transmission electron microscopy (FEI Tecnai G2F20, America FEI,USA) with anacceleration voltage of 200 kV. HAADF-STEM, high-resolution TEM and EELS results were obtained on a JEM-ARM 200F instrument at 200kV. The X-ray diffraction (XRD, X'Pert pro, PANalytical B.V, Netherlands) patterns of the materials were obtained from 30 to 800 with Cu K $\alpha$  radiation ( $\lambda = 0.15406$  nm) at a voltage of 60 kV and a current of 50 mA at a speed of 20 min<sup>-1</sup>. The S  $L_3$ -edge, C  $k$ -edge and N  $k$ -edge XANES measurements were performed at the BL10B beam line of NSRL. X-ray photoelectron spectroscopy (XPS) spectrum was recorded using a Kratos Axis Ultra photoelectron spectrometer (Thermo escalab 250Xi, Thermo Fisher, US) using a monochromatic Al K $\alpha$  source. Linear sweep voltammetry of the S-terminated MoS<sub>2</sub> electrode was carried out using a saturated calomel electrode (SCE) as the reference electrodeand a Pt (Sigma-Aldrich, 99.995%) as the counter electrode. The scan rate was 2 mV s<sup>-1</sup>. Electrochemical studies were carried out using an electrochemical workstation (CHI660E) in a two-electrode system.

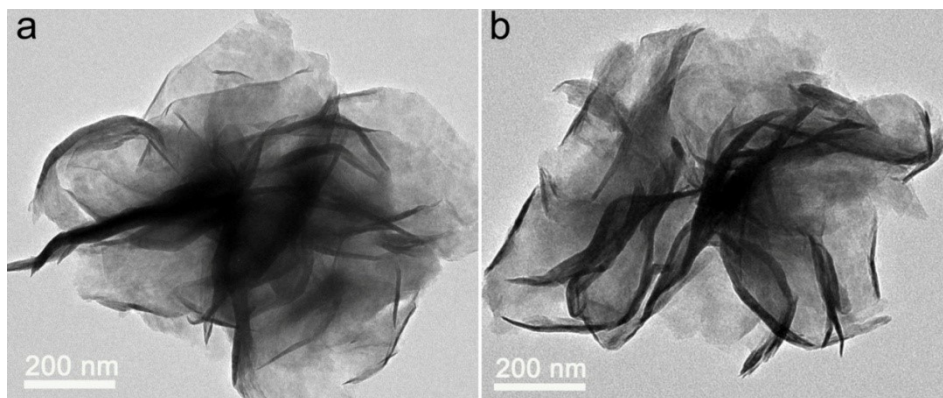


**Figure S1.** TEM image of free-standing pristine MoS<sub>2</sub> and S-terminated MoS<sub>2</sub> nanosheets.

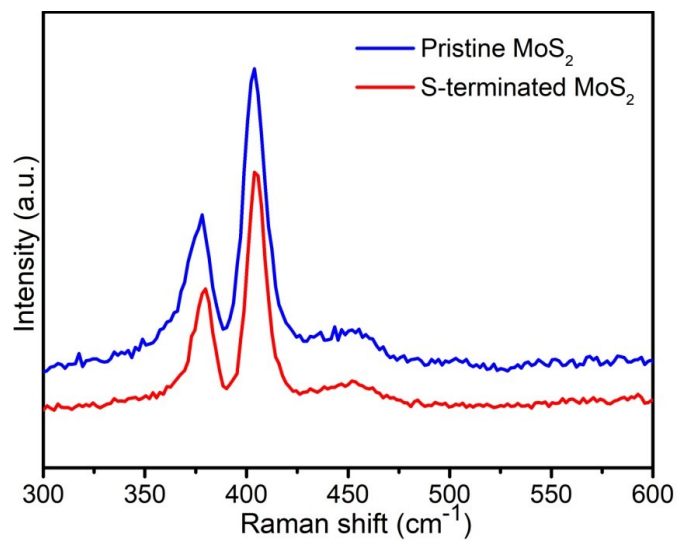


**Figure S2.** Raman spectra of pristine MoS<sub>2</sub> and S-terminated MoS<sub>2</sub> nanosheets.

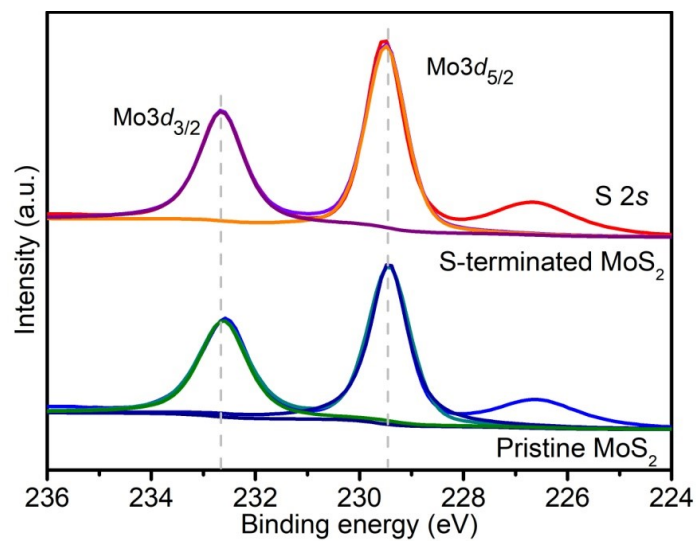


**Figure S3.** Mo 3d XPS spectra of pristine MoS<sub>2</sub> and S-terminated MoS<sub>2</sub> nanosheets.

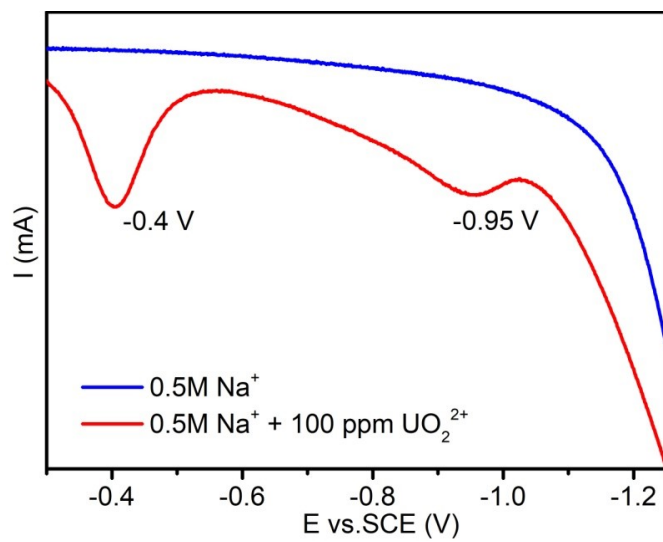


**Figure S4.** LSV curves over S-terminated MoS<sub>2</sub> nanosheets in the presence or absence of U(VI).

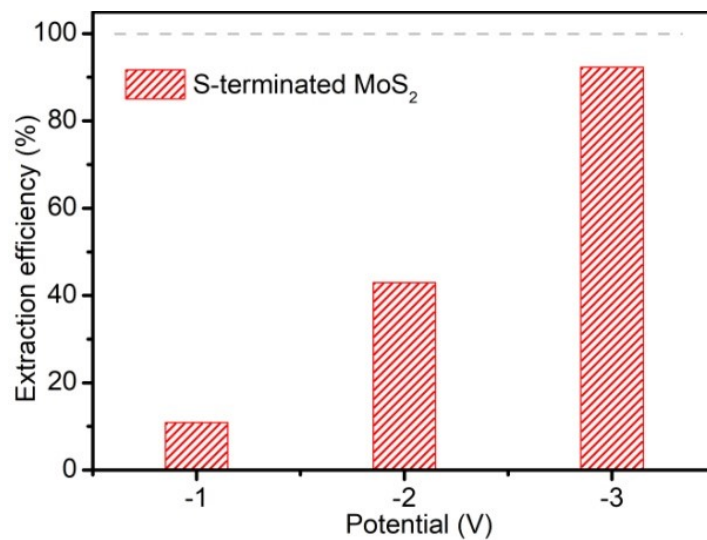


**Figure S5.** The extraction efficiency of S-terminated MoS<sub>2</sub> nanosheets at different voltages in 8 ppm uranium-spiked seawater.

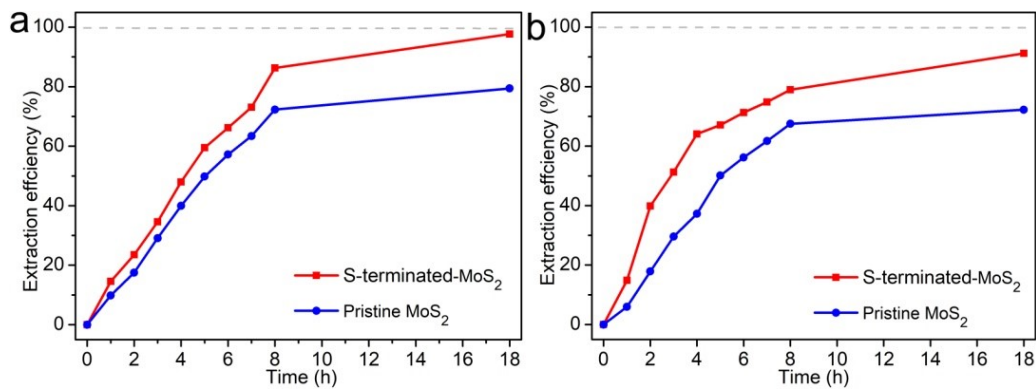


**Figure S6.** (a) Electrochemical extraction efficiency of uranium plot versus the contact time over S-terminated MoS<sub>2</sub> nanosheets in 20 ppm uranium-spiked seawater. (b) Electrochemical extraction efficiency of uranium plot versus the contact time over S-terminated MoS<sub>2</sub> nanosheets in 100 ppm uranium-spiked seawater.



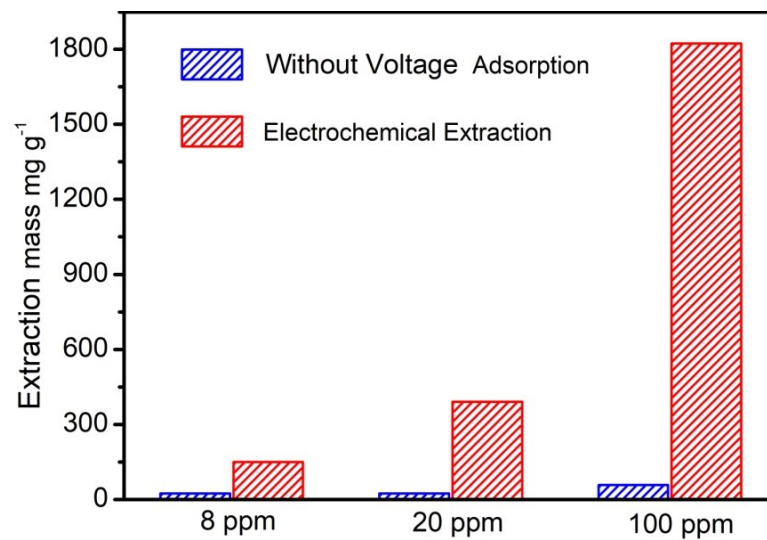


**Figure S7.** Uranium extraction capacity over S-terminated MoS<sub>2</sub> nanosheets in different concentrations of uranium-spiked seawater through using the electrochemical method and the traditional physicochemical method.

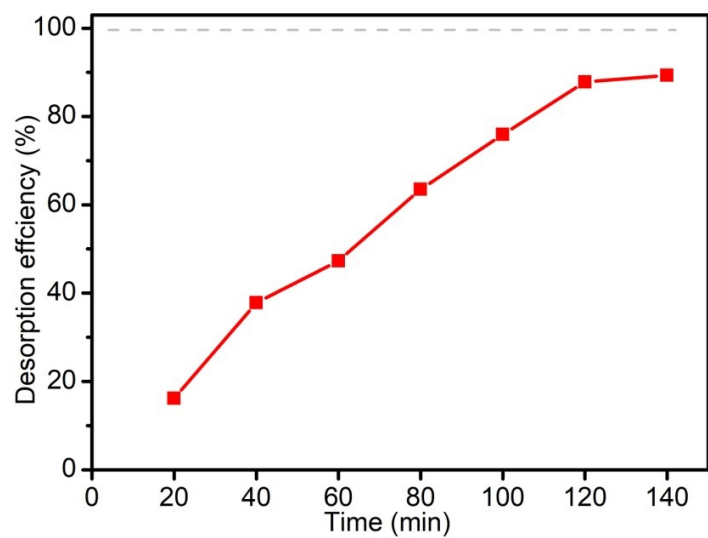


**Figure S8.** The desorption efficiency of uranium in 0.5M of NaNO<sub>3</sub> solution.

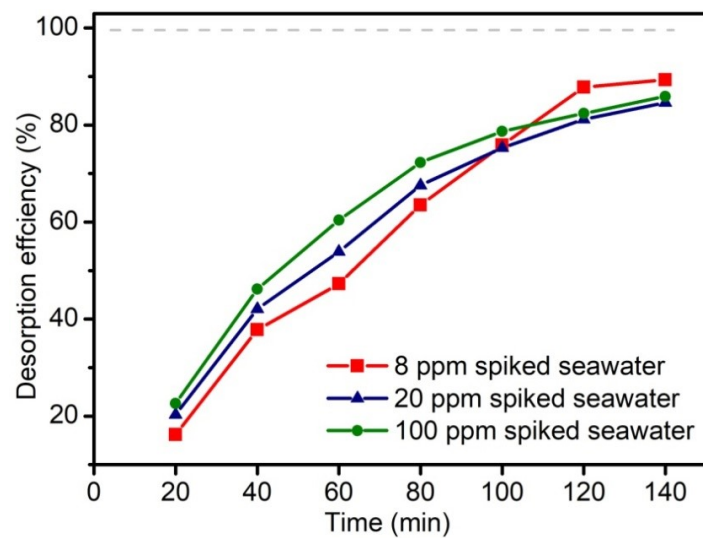


**Figure S9.** The desorption efficiency of uranium in 0.5M of NaNO<sub>3</sub> solution.

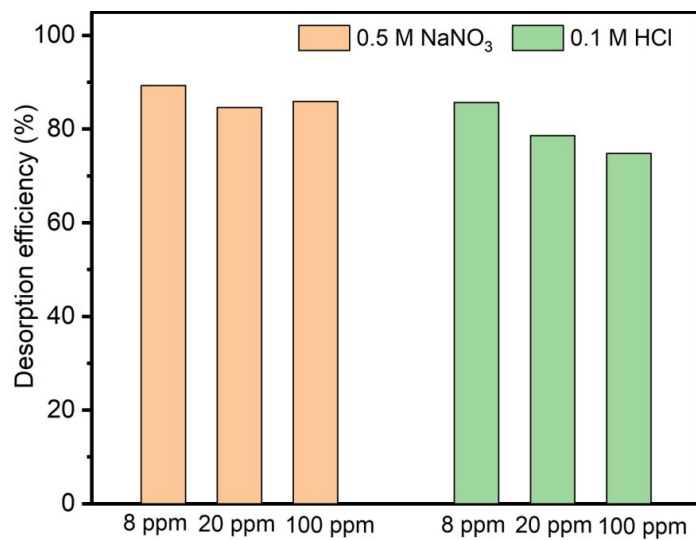


**Figure S10.** Uranium desorption efficiency comparison between different desorption conditions.

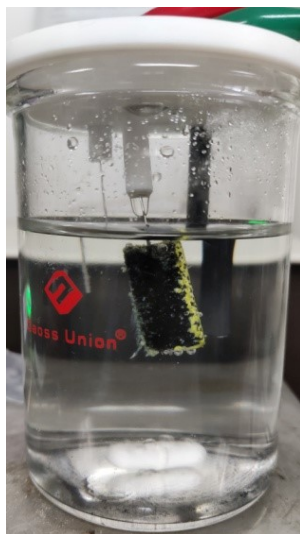


**Figure S11.** The photograph of the electrode after uranium extraction in 100 ppm uranium-spiked seawater.

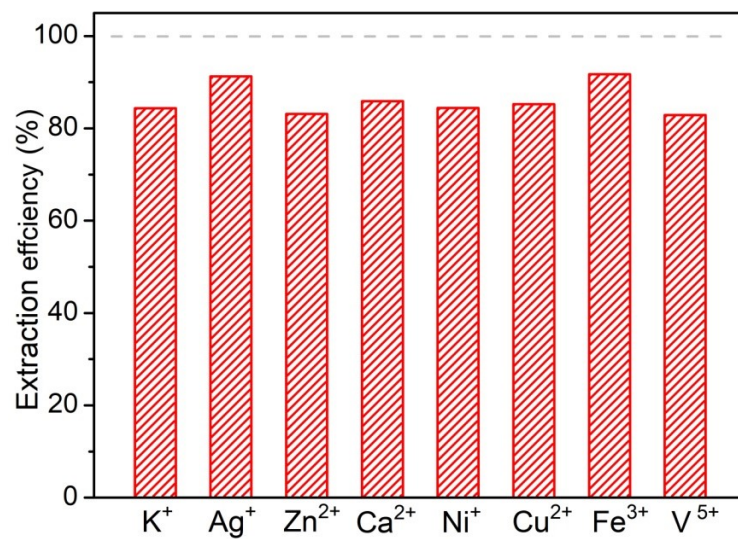


**Figure S12.** The extraction efficiency of S-terminated MoS<sub>2</sub> nanosheets in the presence of individual interfering metal ion in 8 ppm of uranium-spiked seawater.

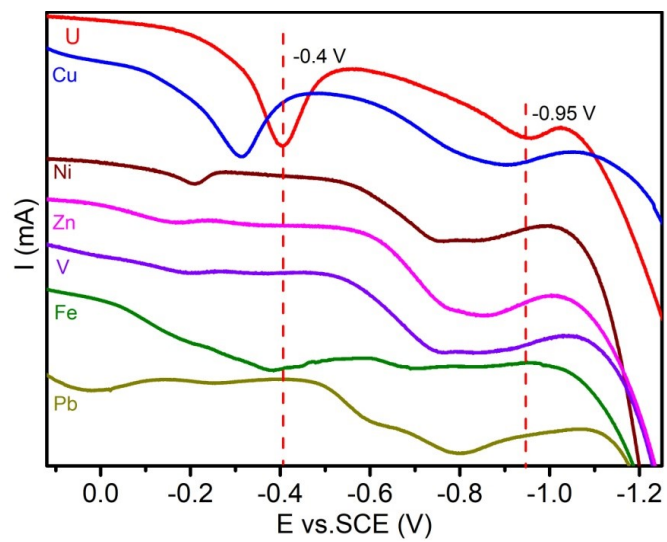


**Figure S13.** LSV curves of interfering metal ion, which indicated the reduction potential.

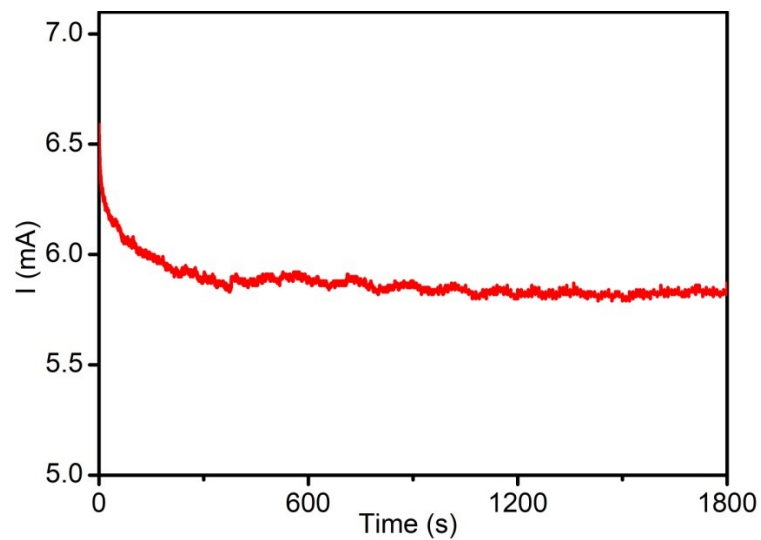


**Figure S14.** The  $i$ - $t$  curve of S-terminated MoS<sub>2</sub> nanosheets in 100 mL of real seawater with 100-time concentrated uranium (330 ppb) over S-terminated MoS<sub>2</sub> nanosheets.



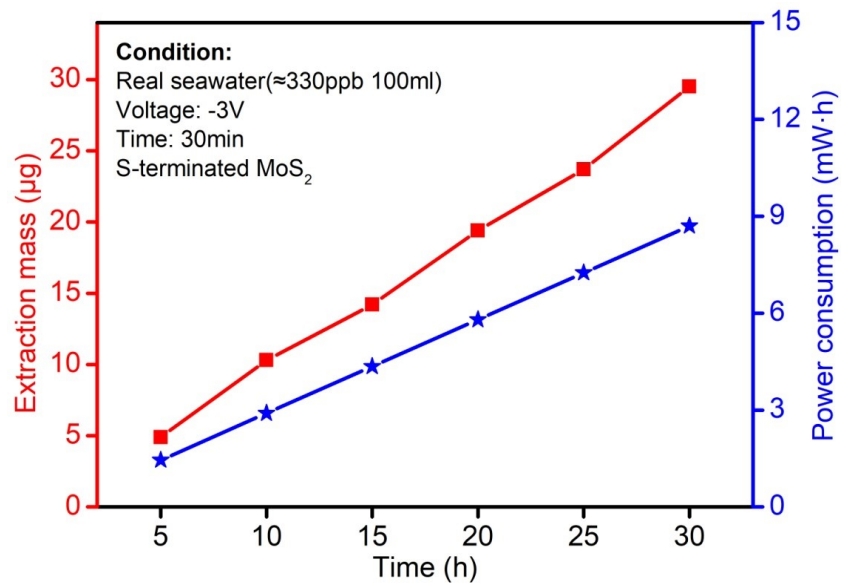


**Figure S15.** Power consumption and extraction mass during 30-min of electrochemical uranium extraction in uranium-concentrated real seawater.

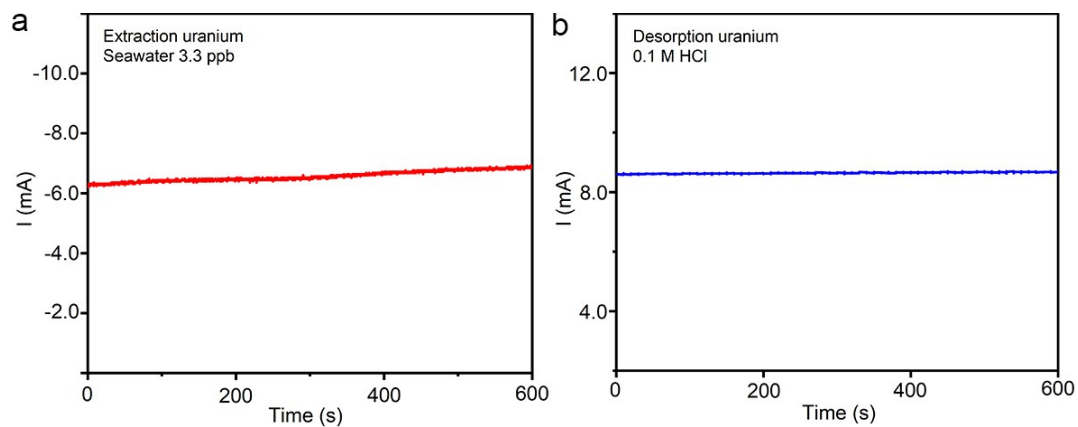


**Figure S16.** The desorption/extraction i-t curve of S-terminated MoS<sub>2</sub> nanosheets in real seawater.

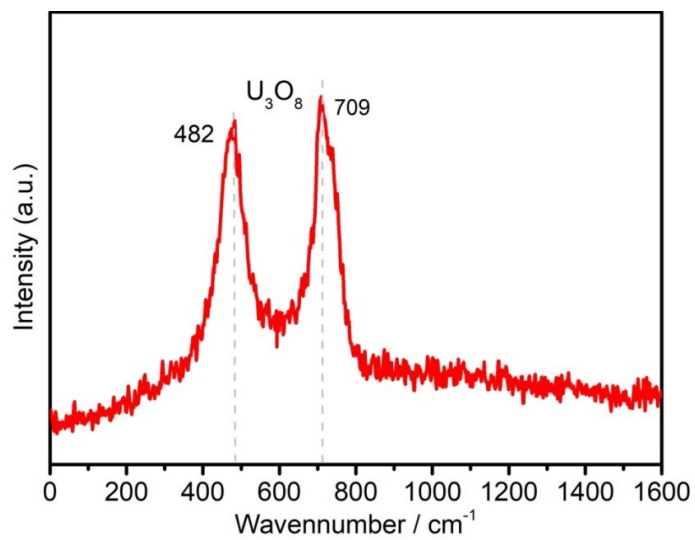


**Figure S17.** Raman spectra of S-terminated MoS<sub>2</sub> nanosheets after uranium extraction.

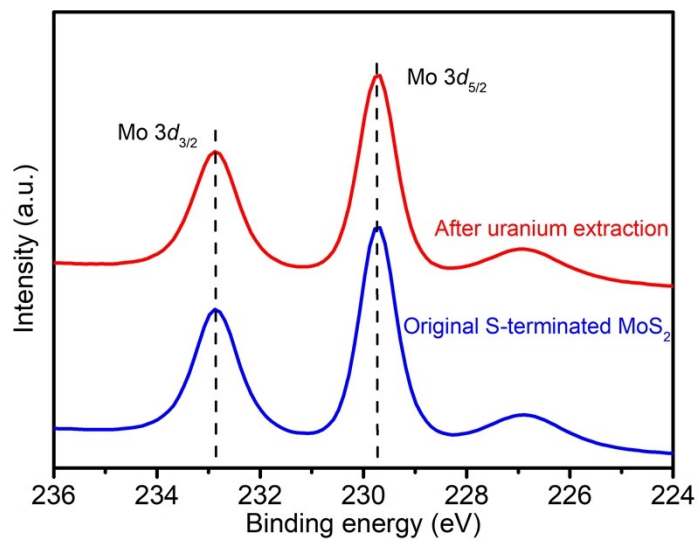


**Figure S18.** Mo 3d XPS spectrum of the S-terminated MoS<sub>2</sub> nanosheets after uranium extraction.

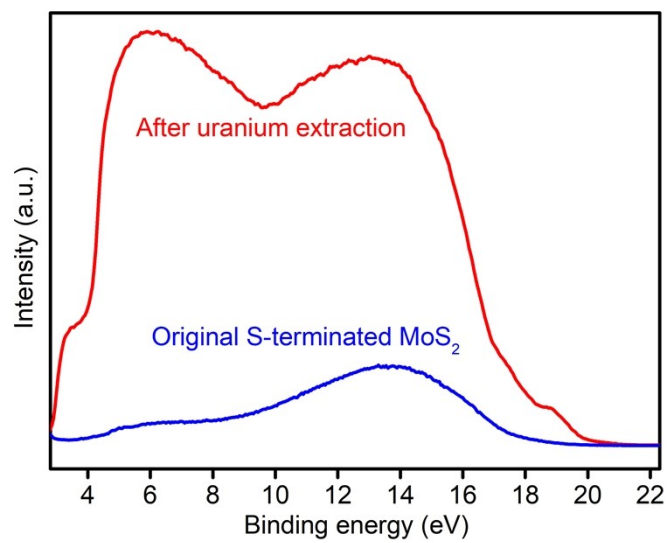


**Figure S19.** The UPS spectra.

**Table S1.** The ion concentration of electrochemical extraction.

Ion species	UO <sub>2</sub> <sup>2+</sup>	V <sup>5+</sup>	Fe <sup>3+</sup>	Co <sup>2+</sup>	Ni <sup>2+</sup>	Cu <sup>2+</sup>	Pb <sup>2+</sup>	Ca <sup>2+</sup>	Zn <sup>2+</sup>
Concentration (ppb)	330	152	141	5.3	101	65	34.6	60000	408
Electrochemical extraction (ppb)	294.7	6.4	32.6	0.22	30.2	26.8	1.6	1416	127.7

## Reference:

- [1] J. F. Xie, H. Zhang, S. Li, R. X. Wang, X. Sun, M. Zhou, J. F. Zhou, X. W. Lou, Y. Xie, *Adv. Mater.* **2013**, 25, 5807-5813.
- [2] Kresse, G., and Furthmüller, J. (1996). Efficiency of Ab-Initio Total Energy Calculations for Metals and Semiconductors Using a Plane-Wave Basis Set. *Comput. Mater. Sci.* 6, 15-50.
- [3] J. P. Perdew, K. Burke, M. Ernzerhof, *Phys. Rev. Lett.* **1996**, 77, 3865-3868.
- [4] a) P. E. Blöchl, *Phys. Rev. B: Condens. Matter Mater. Phys.* **1994**, 50, 17953-17979; b) G. Kresse, D. Joubert, *Phys. Rev. B: Condens. Matter Mater. Phys.* **1999**, 59, 1758-1775.
- [5] H. J. Monkhorst, J. D. Pack, *Phys. Rev. B* **1976**, 13, 5188-5192.
- [6] S.Grimme, J. Antony, S. Ehrlich, H. Krieg, *J. Chem. Phys.* **2010**, 132, 154104.